

PROCEEDINGS OF SPIE

[SPIDigitalLibrary.org/conference-proceedings-of-spie](https://spiedigitallibrary.org/conference-proceedings-of-spie)

Multidimensional light field manipulation and applications based on optical metasurface

Li, Tianyue, Fu, Boyan, Ren, Jianzheng, Wang, Shuming, Wang, Zhenlin, et al.

Tianyue Li, Boyan Fu, Jianzheng Ren, Shuming Wang, Zhenlin Wang, Shining Zhu, "Multidimensional light field manipulation and applications based on optical metasurface," Proc. SPIE 11850, First Optics Frontier Conference, 1185004 (18 June 2021); doi: 10.1117/12.2598880

SPIE.

Event: First Optics Frontier Conference, 2021, Hangzhou, China

Multidimensional light-field Manipulation and Applications Based on Optical Metasurface

Tianyue Li^a, Boyan Fu^a, Jianzheng Ren^a, Shuming Wang^{*a, b}, Zhenlin Wang^a, Shining Zhu^{a, b}

^a National Laboratory of Solid-State Microstructures, School of Physics, Nanjing University, Nanjing, China, 210093;

^b Key Laboratory of Intelligent Optical Sensing and Manipulation Ministry of Education, Nanjing, China, 210093.

ABSTRACT

Metasurface is a class of two-dimensional microstructure functional materials, which has an ability of modulating light in subwavelength region and becomes a hot topic during the last decade. An advantage of metasurfaces is their versatility by invoking the degrees of freedom of light field to achieve various functionalities. In this paper, we report methods of using the polarization and dispersion of light to achieve multifunctional metasurface devices, allowing the different degrees of freedom of light to carry independent phase profiles to achieve the polarization-dependent conversion of Bessel beams with different orders and numerical apertures as well as integrated optical tweezers-optical spanner metasurface. Also, the wavelength-controlled multifunctional metalens by introducing an improved genetic algorithm has been implemented. We envision our research are expected to be the potential candidates in multifunctional integrated optical devices.

Keywords: Metasurface, Metalens, Light-field manipulation, Bessel beams, Optical tweezers, Optical spanner

1. INTRODUCTION

Metasurfaces is the counterpart of two-dimensional metamaterials, comprised of subwavelength nano-antennas, which can flexibly control the phase, amplitude and polarization of light field, and are successfully applied in imaging, communication, displaying etc [1-2]. With the development of micro-nano manufacture, how to modulate light-field in multidimension and integrate more functions into one ultracompact device becomes a topic of concern. Primarily, the geometric phase (i.e., Pancharatnam – Berry phase) and the dynamic phase are two basic mechanisms for modulating the phase and amplitude. Here, by the interplay of combining the geometric phase and the dynamic phase, we propose a method to decouple the spin eigenstates in quantum optics corresponded to the orthogonal polarization in wave optics to realize the conversion of Bessel beams with different orders and numerical apertures (NAs) with different polarized light incidence. The tight focus effect caused by the high NA in the process of changing the incident polarization state and the accompanying spin-orbit angular momentum conversion will introduce the longitudinal component, leading to the singularity of the spot is observed and studied. By using the same principle, we design an integrated optical tweezers (OT) – optical spanner (OS) metasurface under the incidence of linearly polarized light in the visible, and then the PS sphere acts as a probe to verify the trapping and rotation micro-manipulation capabilities. In terms of dispersion, we use an improved genetic algorithm to arrange the three centrosymmetric nano-structures so that the dynamic-phase-only of the structures can fit the theoretical phase in the phase space as much as possible. For a proof-of-concept, we give the demonstrations of color-router guiding four different wavelengths and a triple multiplexing Metalens, which emits the focused beam, Bessel beam with NA=0.6 and focused orbital angular momentum (OAM). Our results are expected to play an important role in multifunctional integrated optical devices.

[*wangshuming@nju.edu.com](mailto:wangshuming@nju.edu.com);

2. GENERATION AND CONVERSION DYNAMICS OF DUAL-BESSEL BEAMS

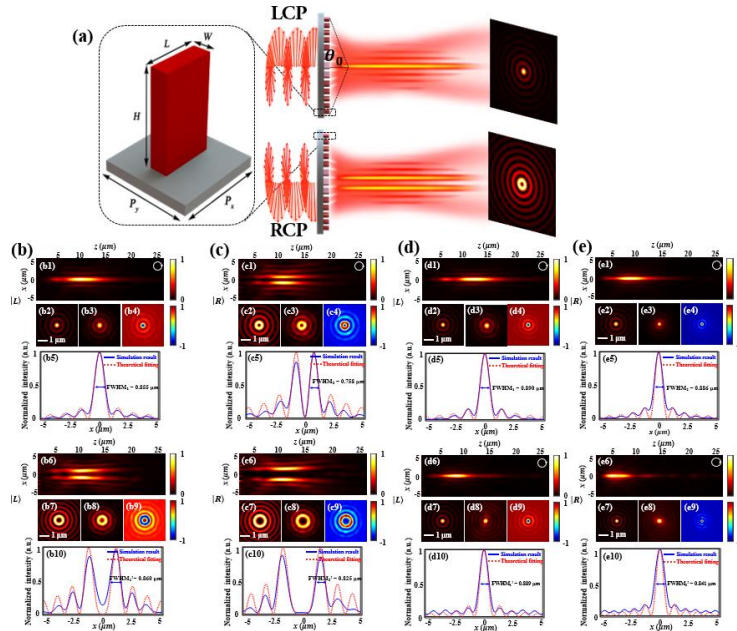


Figure 1. (a) Schematic diagram of polarization-dependent Bessel beam generator. Theoretical calculation and simulation results of Bessel beams with independent orders (b),(c). Theoretical calculation and simulation results of Bessel beams with different NAs (d),(e).

Bessel beam is a structural beam with non-diffraction and self-healing properties, which has attracted a lot of research interest, and been widely used in the fields of artificial black hole generation, super-resolution imaging, and optical pulling forces. In recent years, due to the difficulty of generating high NA Bessel beam in the bulky materials and complex optical systems, researchers prefer to use planar optical elements such as metasurface to generate Bessel beams. In this section, we introduce a method to emit Bessel beams with different orders and NAs by means of orthogonal polarization states incidence, respectively.

polarization-dependent Bessel beams generator depicts in Figure 1(a). In order to make the metasurface device have different optical responses with the orthogonal polarization states normally incident onto metasurface, the following phase profiles must be satisfied:

$$\varphi^+(x, y) = -\frac{2\pi}{\lambda} \sqrt{x^2 + y^2} \cdot NA_1 + n\phi \quad (1)$$

$$\varphi^-(x, y) = -\frac{2\pi}{\lambda} \sqrt{x^2 + y^2} \cdot NA_2 + (n+1)\phi \quad (2)$$

where x, y represent the position of each nano-structure, λ is the working wavelength in free space and we set $\lambda = 1550$ nm, NA_i is the numerical aperture of the metasurface, n is the order of Bessel beams and $\phi = \arctan(y/x)$ is the azimuthal angle which represents the higher-order Bessel beam imparted by the optical vortex. The principle of different orthogonal polarization states carrying different phases can be found in Ref. [3]. Through our design, we keep the parameter $NA_1 = NA_2 = 0.4$, and demonstrate the orders $n_1 = 0$ and $n_2 = 1$ for case 1, $n'_1 = 2$ and $n'_2 = 3$ for case 2 using two samples with $R = 12$ μm as well as $NA_1 = 0.4$, $NA_2 = 0.6$ for case 3, $NA_1' = 0.6$, $NA_2' = 0.8$ for case 4 using two samples with $R = 20$ μm . The results are shown in Fig. 1(b)-(e). Figure 2(a) and 2(b) shows the conversion dynamics of transverse pattern with polarization angle δ from $-\pi/2$ to $\pi/2$ can be shown on the Poincaré Sphere. One can see that the singularity of the spot in both cases splits in three parts from the center and gradually extend outward to three parts, which is associated

with the tight focusing effect, leading to the conversion from spin angular momentum (SAM) to orbital angular momentum. For tight focusing, the spin-to-orbit conversion leads to the following relation:

$$\begin{aligned} |L\rangle &\rightarrow e^{i(n-2)\phi} |L\rangle + e^{in\phi} |R\rangle + e^{i(n-1)\phi} |z\rangle \\ |R\rangle &\rightarrow e^{i(n+3)\phi} |R\rangle + e^{i(n+1)\phi} |L\rangle + e^{i(n+2)\phi} |z\rangle \end{aligned} \quad (3)$$

where $|L\rangle$, $|R\rangle$, $|z\rangle$ represent the left circularly polarization (LCP), right circularly polarization (RCP) and longitudinal component, respectively. Due to the presence of the geometric phase, only the cross polarization of the output field needs to be considered (i.e., $e^{in\phi} |R\rangle \gg e^{i(n-2)\phi} |L\rangle$, $e^{i(n+1)\phi} |L\rangle \gg e^{i(n+3)\phi} |R\rangle$) and the longitudinal component has the same magnitude and the interference is the most significant for linearly polarized (LP) state incidence, which leads to the singularity of the patterns. Fig. 2(c) and 2(e) shows the longitudinal component of the transverse pattern with linearly polarization incidence [4].

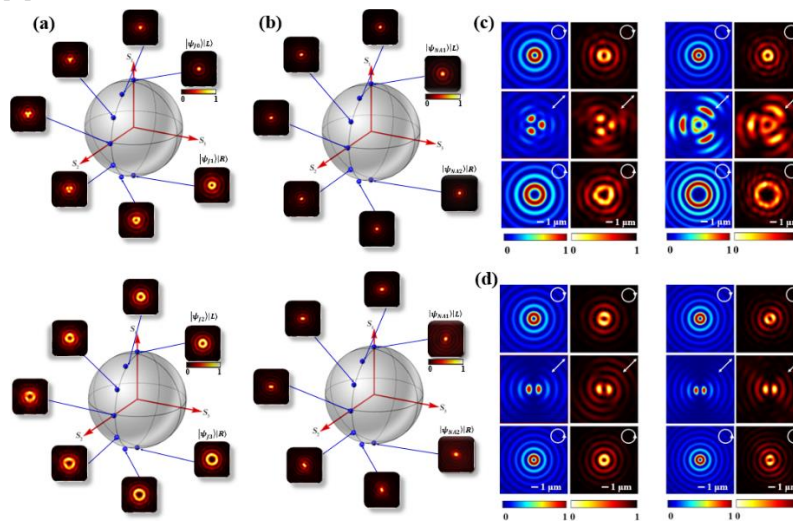


Figure 2. (a),(b) Snapshots of transverse patterns for different incident polarizations on the path of Poincaré sphere. Theoretical calculation (left) and simulation results (right) of longitudinal component of Bessel beam with independent orders (c) and different NAs (d) for LCP, LP and RCP incidence.

3. INTEGRATED OT-OS METASURFACE

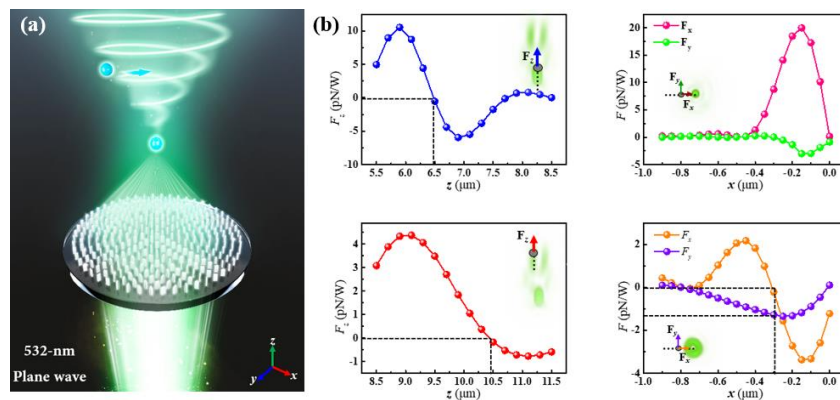


Figure 3. (a). Schematic diagram of the integrated OT-OS metasurface. (b). Calculated optical forces on a PS particle located in the vicinity of the focusing spot (left) and the vortex field (right).

According to the principles discussed in Ref. [3], we have integrated the OT and OS into an individual metasurface device at $\lambda = 532$ nm in the visible regime [5]. Figure 3(a) schematically illustrates the OT-OS metasurface device, and the phase profiles of OT and OS must be introduced as follows:

$$\phi^+(x, y, f_{OT}) = -2\pi(\sqrt{x^2 + y^2 + f_{OT}^2} - f_{OT})/\lambda \quad (4)$$

$$\phi^-(x, y, f_{OS}) = -2\pi(\sqrt{x^2 + y^2 + f_{OS}^2} - f_{OS})/\lambda + l\varphi \quad (5)$$

where (x, y) denotes the coordinate of each nano-structures on the metasurface, and f_{OT} and f_{OS} are the focal lengths for each response. Also, an additional vortex term $l\varphi$ in Eq. (5) is required for the phase profile of the OS, where l denotes topological charge. To verify the manipulation ability of the OT-OS metasurface, Finite-difference time domain (FDTD) simulations were performed by using a polystyrene (PS) nanosphere (radius: $R_{PS}=100$ nm; $n_{PS}=1.59$) as a probe. The optical force is rigorously calculated by the Maxwell's stress tensor method [6]. Fig. 3(b)-(e) shows the calculated force exerted on the particle located at different positions on the $y = 0$ plane. When the particle is close to the tight focusing spot, three dimensional trapping occurs at $x = 0$ and $z = 6.5$ μm , as shown in Fig. 3(b) and (c). Notice that in Fig. 3(b) the appearance of a small y -component force when the particle deviates from the equilibrium position, which should be influenced by the Belinfante's spin current due to spin inhomogeneity. By contrast, when the particle is located around the OS, the zero points of the x - and z -component forces arise around $x = -0.4$ μm and $z = 10.4$ μm , as shown in Fig. 3(d) and (e).

so far, we show the possibility of integrating the OT and OS onto one identical single-layer metasurface. The mechanism is the coexisting geometric and dynamic phases, which confer two kinds of polarization-dependent optical responses upon the metasurface. Additionally, since the two optical responses are independent of each other, the focal planes of the tweezers and spanner can be flexibly tailored.

4. WAVELENGTH-CONTROLLED MULTIFUNCTIONAL METALENSSES

Compared with devices we show above, the wavelength-controlled multifunctional metalenses mainly utilize several distinct wavelengths to manipulate the phase profile. Since the geometric phase depends on the rotation angle of each nano-structures, which cannot cover more than two arbitrary phase profiles. Therefore, we show something in old fashion that the dynamic-phase-based metalens with centrosymmetric nano-structures occupied the whole phase space can fit the theoretical phase values as much as possible with multiple wavelengths.

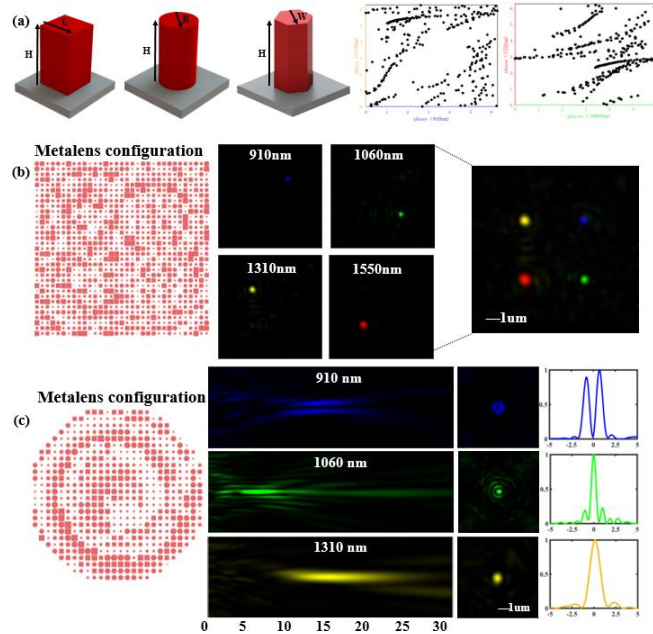


Figure. 4. (a). Three centrosymmetric nano-structures with their actual phase shifts. (b). color router based on Metalens with four independent wavelength channels. (c). trifunctional Metalens with a focused OAM, a Bessel beam and a focused beams generation

We begin by choosing three basic types of nano-structures with cross sections of rectangular, circular and hexagonal (Figure. 4(a)). In this way, the actual dynamic phases of the structures are more in the phase space of $0-2\pi$. Then, we use

the optimized genetic algorithm to fill each structure with the smallest residual difference from the theoretical value into the metasurface to obtain the desired wavelength-controlled metalens. Fig. 4(b) shows a multiplex color router with dielectric metalens, which is capable of guiding four wavelengths (910 nm, 1060 nm, 1310 nm, 1550 nm) into different spatial pixels, the focusing efficiency within each pixel is more than 24.8%. Fig. 4(c) shows a wavelength-dependent trifunctional metalens for a focused OAM, a Bessel beam and a focused beams generation, respectively. Each generation efficiency of each beam is at least 30%.

5. CONCLUSION AND OUTLOOK

Overall, we introduce two kinds of multifunctional metasurface devices controlled by polarization and wavelength, respectively. Specifically, the firstly introduced Bessel beams generator will produce the singularity of the transverse pattern due to the spin-orbit interaction caused by the longitudinal component with LP incidence. Next the OT-OS metasurface devices proves the PS nanosphere can be trapped and rotated on the different focal planes along the optical axes. And finally the wavelength-controlled metalenses have been numerically demonstrated so that the three or four functionalities can be achieved by varying the incident wavelength. Our research may offer a way for constructing compact photonic platform ranging from structural beams generation toward optical manipulation in subwavelength region.

REFERENCES

- [1]. S. Wang, P. C. Wu, V. C. Su, Y. C. Lai, C. H. Chu, J. W. Chen, S. H. Lu, J. Chen, B. Xu, C. H. Kuan, T. Li, S. Zhu, D. P. Tsai., "Broadband achromatic optical metasurface devices," *Nat. Commun. Papers* 8, 187 (2017)
- [2]. S. Wang, P. C. Wu, V. Su, Y. Lai, M. Chen, H. Y. Kuo, B. H. Chen, Y. H. Chen, T. Huang, J. Wang, R. Lin, C. Kuan, T. Li, Z. Wang, S. Zhu and D. P. Tsai., "A broadband achromatic metalens in the visible," *Nat. Nanotechnol. Papers* 13, 227 (2018).
- [3]. J. P. Balthasar Mueller, N. A. Rubin, R. C. Devlin, B. Groever and F. Capasso., "Metasurface polarization optics: Independent phase control of arbitrary orthogonal states of polarization," *Phys. Rev. Lett. Papers* 118 (11), 113901 (2017).
- [4]. T. Li, X. Li, S. Yan, X. Xu, S. Wang, B. Yao, Z. Wang, and S. Zhu., "Generation and Conversion Dynamics of Dual Bessel Beams with a Photonic Spin-Dependent Dielectric Metasurface," *Phys. Rev. Appl. Papers* 15 (1), 014059 (2021).
- [5]. T. Li, X. Xu, B. Fu, S. Wang, B. Li, Z. Wang, S. Zhu., "Integrating the optical tweezers and spanner onto an individual single-layer metasurface," *Photonics. Res. Papers* 9 (6)
- [6]. J. D. Jackson., [Classical Electrodynamics,3rd ed], Wiley Publishers,(1998).